Dalton Transactions

RSCPublishing

PERSPECTIVE

View Article Online

Cite this: Dalton Trans., 2013, 42, 15846

Long-lived photoinduced charge separation for solar cell applications in supramolecular complexes of multi-metalloporphyrins and fullerenes

Shunichi Fukuzumi*a,b and Kei Ohkuboa

Monomers, dimers, trimers, dendrimers and oligomers of metalloporphyrins form supramolecular complexes with fullerene derivatives via electrostatic interactions, π - π interactions and coordination bonds. Photoexcitation of the supramolecular complexes resulted in photoinduced electron transfer from the porphyrin moiety to the fullerene moiety to produce the charge-separated states as revealed by laser flash photolysis measurements. The rate constants of photoinduced charge separation and charge recombination in supramolecular complexes of multi-metalloporphyrins and fullerenes were also determined by laser flash photolysis measurements and the results depending on the number of porphyrins in the supramolecular complexes are discussed in terms of efficiency of photoinduced energy transfer and charge separation as well as the lifetimes of charge-separated states. The photoelectrochemical performances of solar cells composed of supramolecular complexes of monomers, dimers, dendrimers and oligomers of metalloporphyrins with fullerenes are compared in relation to the rate constants of photoinduced charge separation and charge recombination.

Received 12th July 2013, Accepted 3rd October 2013 DOI: 10.1039/c3dt51883c

www.rsc.org/dalton

^aDepartment of Material and Life Science, Division of Advanced Science and Biotechnology, Graduate School of Engineering, Osaka University, ALCA, Japan Science and Technology Agency (JST), Suita, Osaka 565-0871, Japan. E-mail: fukuzumi@chem.eng.osaka-u.ac.jp; Fax: +81-6-6879-7370; Tel: +81-6-6879-7368

1. Introduction

Photosynthesis is one of the most fundamental and indispensable processes in nature, because it converts light energy into chemical energy required to maintain life.^{1,2} Photosynthesis is initiated by the multistep electron-transfer reactions in the photosynthetic reaction centres following light energy harvesting by antenna chlorophylls, funnelled to a bacteriochlorophyll



Shunichi Fukuzumi

Shunichi Fukuzumi earned a Ph.D. degree in applied chemistry at the Tokyo Institute of **Technology** in 1978. After working as a postdoctoral fellow (1978-1981) at Indiana University in USA, he joined the Department of Applied Chemistry, Osaka University, as an Assistant Professor in 1981 and was promoted to a Full Professor in 1994. He is now a special distinguished professor at Osaka University and the director of an ALCA (Advanced Carbon Technology Research and Development) project that started in 2011.



Kei Ohkubo

Kei Ohkubo earned his Ph.D. degree from the Graduate School of Engineering, Osaka University in 2001. He was working as a JSPS fellow and a JST research fellow at Osaka University from 2001 to 2005. He has been a designated associate professor at Osaka University since 2005.

^bDepartment of Bioinspired Science, Ewha Womans University, Seoul 120-750, Korea

Dalton Transactions

dimer, the so-called special pair, to attain the long-lived charge-separated (CS) state. 1,2 The redox-active components such as chlorophyll, pheophytin and quinones are appropriately located in the protein matrix by non-covalent interactions.1,2 Extensive efforts have so far been devoted to the design of electron donor-acceptor composites using covalently and non-covalently linked systems to form the long-lived CS state upon photoexcitation for artificial photosynthesis. 3-29 Porphyrins, which are involved in a number of important bio-

logical electron-transfer systems including the primary photochemical reactions of chlorophylls (porphyrin derivatives) in the photosynthetic reaction centres, are particularly attractive building blocks as electron acceptors as well as light-harvesting compounds for the construction of supramolecular electron donor-acceptor composites due to their excellent photophysical and electron-transfer properties.8-29 With regard to electron acceptors, fullerenes, which are extensively conjugated three-dimensional π systems, are ideal electron acceptors because of the minimal changes of structure and solvation associated with the electron-transfer reduction. 30-38 Thus, combination of porphyrins and fullerenes is regarded as ideal donor-acceptor ensembles, because the combination results in a small reorganization energy, which allows to accelerate photoinduced electron transfer and to slow down charge recombination, leading to the generation of long-lived CS states with high quantum yields. 39-63 However, non-covalent binding between monomer porphyrins and fullerenes is usually not strong enough in polar solvents which are generally used for studies on photoinduced electron-transfer reactions. 64-68 Among non-covalent interactions, an electrostatic interaction is relatively strong in polar solvents.^{69–73} Muti-point binding sites can be introduced by using multimetalloporphyrins (dimers, trimers, dendrimers and oligomers), allowing strong binding between multi-metalloporphyrins and fullerenes in polar solvents. 29,30

In this perspective, we review our recent development on photoinduced charge separation in supramolecular complexes of porphyrin anions and fullerene cations with electrostatic interactions and those composed of multi-metalloporphyrins and fullerenes, which are strongly bound in polar solvents, towards construction of supramolecular solar cells based on the long-lived photoinduced charge separation.

Supramolecular complexes of monomer porphyrin sulfonates and Li⁺@C₆₀

Zinc tetraphenylporphyrin tetrasulfonate anion [(Bu₄N⁺)₄-ZnTPPS⁴⁻] forms a strong supramolecular binding with a cationic lithium ion encapsulated fullerene (Li⁺@C₆₀)⁷⁴⁻⁷⁷ in benzonitrile (PhCN) by electrostatic and π - π interactions (Scheme 1).⁷⁸ The Job's plots of the absorbance change confirmed the 1:1 stoichiometry between ZnTPPS4- and Li⁺@C₆₀. 78 Free base tetraphenylporphyrin tetrasulfonate anion [(Bu₄N⁺)₄H₂TPPS⁴⁻] also forms a 1:1 complex with $Li^{+} \otimes C_{60}$. The formation constants (K) of the ZnTPPS⁴⁻/ $Li^{+} \otimes C_{60}$ and H₂TPPS⁴⁻/Li⁺(a)C₆₀ complexes were determined from the absorption change to be 1.6×10^5 and 3.0×10^5 M⁻¹, respectively.⁷⁸ The same formation constants were obtained from the fluorescence quenching of ZnTPPS4- and H2TPPS4- and by Li⁺@C₆₀ in PhCN.⁷⁸

The occurrence of the photoinduced energy transfer in the supramolecular complex was confirmed by the transient absorption spectra of the ZnTPPS⁴⁻-Li⁺@C₆₀ complex measured in PhCN using femtosecond laser flash photolysis (Fig. 1a).⁷⁸ The transient absorption bands taken at 2 ps observed at 620 and 737 nm are assigned to the singlet excited state of ZnTPPS4-. This band decays with the rate constant $(k_{\rm EN})$ of $9.7 \times 10^{10} \, {\rm s}^{-1}$ (Fig. 1b) to form the singlet excited state of Li⁺@C₆₀ at 100 ps (Fig. 1a). The decay rate constant of $^{1}[\text{Li}^{+}@\text{C}_{60}]^{*}$ was determined to be $8.9 \times 10^{8} \text{ s}^{-1}$, which agrees with the rate constant of the intersystem crossing of Li⁺@C₆₀.⁷⁸ Thus, efficient energy transfer occurred from 1 [ZnTPPS $^{4-}$]* to Li $^{+}$ @C₆₀ rather than electron transfer.

The transient absorption spectra taken by nanosecond laser flash photolysis shown in Fig. 2a demonstrate the formation of $[ZnTPPS^{4-}]^{*+}$ (λ_{max} = 670 nm) and that of $Li^{+}@C_{60}$ radical anion (λ_{max} = 1035 nm).⁷⁸ Thus, the electron transfer from



Scheme 1 Supramolecular complex formation and photoinduced charge separation of MTPPS⁴⁻ (M = Zn and H₂) with Li⁺@C₆₀ in PhCN.

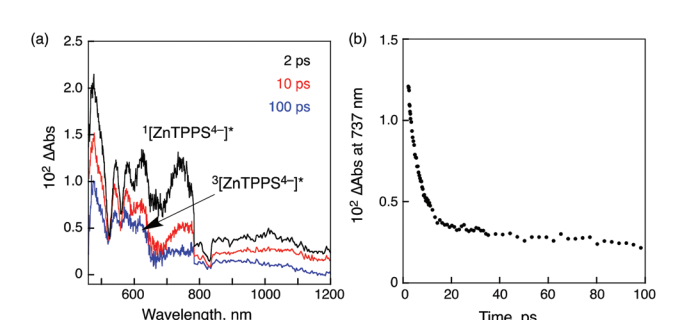


Fig. 1 (a) Transient absorption spectra of ZnTPPS⁴⁻ (2.5×10^{-5} M) in the presence of Li⁺@C₆₀ (5.0×10^{-5} M) in deaerated PhCN at 298 K taken at 2, 10 and 100 ps after femtosecond laser excitation at 388 nm. (b) Time profile at 737 nm.

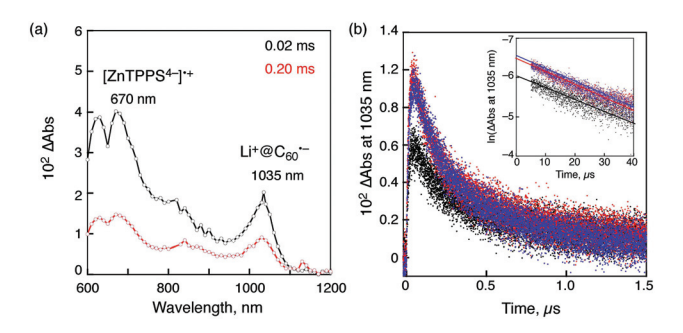


Fig. 2 (a) Transient absorption spectra of ZnTPPS⁴⁻ (2.5×10^{-5} M) in the presence of Li⁺@C₆₀ (5.0×10^{-5} M) in deaerated PhCN at 298 K taken at 20 and 200 μ s after nanosecond laser excitation at 550 nm; (b) decay time profiles at 1035 nm with different laser intensities (1, 3, 6 mJ per pulse). Inset: first-order plots.

ZnTPPS⁴⁻ to ${}^3[\text{Li}^+@\text{C}_{60}]^*$ or from ${}^3[\text{ZnTPPS}^{4-}]^*$ to $\text{Li}^+@\text{C}_{60}$ occurs in the supramolecular complex to produce the triplet charge-separated (CS) state. The lifetime of the triplet CS state of the supramolecular complex was determined to be 300 μ s for ZnTPPS⁴⁻ from the first-order decay of the CS state (Fig. 2b). The supramolecular complex because the first-order decay rate constant remains the same irrespective of the difference in the laser intensity (inset of Fig. 2b). Similarly the CS lifetime of 310 μ s was determined for [(H₂TPPS⁴⁻)*-Li*@C₆₀*-]. This is the longest lifetime of the CS state ever reported for monomer porphyrin/fullerene systems linked non-covalently in solution. The quantum yield of the CS state is determined to be 0.39 using the absorption of the CS state (Li*@C₆₀*-: ε ₁₀₃₅ = 7300 M⁻¹ cm⁻¹).

The activation enthalpies of the charge-recombination (CR) processes were determined to be 3.0 kcal mol $^{-1}$ for ZnTPPS $^{4-}$ Li $^{+}$ @C $_{60}$ and 5.4 kcal mol $^{-1}$ for H_2TPPS^{4-} Li $^{+}$ @C $_{60}$. This indicates that there is a significant energy difference between the singlet and triplet CS states and that the CR processes may occur through the thermally activated singlet CS state. The lifetime of the CS state at 77 K is estimated as long as 60 h for H_2TPPS^{4-} Li $^{+}$ @C $_{60}$. Such a long-lived triplet CS state was detected by the EPR measurements by photoirradiation of the H_2TPPS^{4-} Li $^{+}$ @C $_{60}$ complex in frozen PhCN as shown in

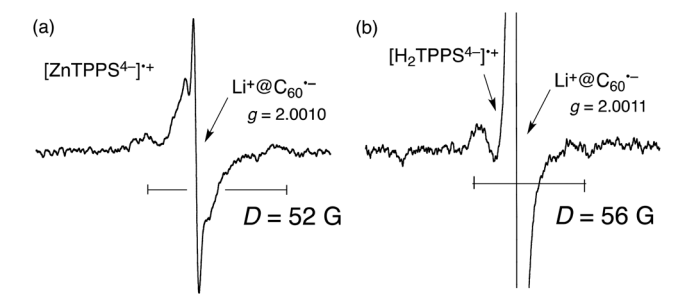


Fig. 3 EPR spectra of (a) $(ZnTPPS^{4-})^{++}-Li^{+}@C_{60}^{--}$ and (b) $(H_2TPPS^{4-})^{++}-Li^{+}@C_{60}^{--}$ in PhCN generated by photoirradiation with a high-pressure Hg lamp (1000 W) at 77 K.

Fig. 3. The spin–spin interaction in the triplet radical ion pair of the supramolecular complex is clearly shown at 77 K, where the fine structure due to the triplet CS state is clearly observed at g=2. From the zero-field splitting values (D=52 G for ZnTPPS⁴⁻ and 56 G for H₂TPPS⁴⁻) the distances (r) between two electron spins were estimated using the relation, $D=27\,800/r^3$, ^{79,80} to be 8.1 and 7.9 Å, respectively. ⁷⁸ These r values agree with the centre-to-centre distance of a reported crystal structure of porphyrin/C₆₀.

By mixing PhCN solutions of the supramolecular complexes of MTPPS^{4–} and Li⁺@C₆₀ with acetonitrile (MeCN), nanoclusters were produced and they were deposited on an optically transparent electrode (OTE) of nanostructured SnO₂ (OTE/SnO₂) by application of a dc electric field (\sim 100 V cm⁻¹) to construct photovoltaic cells. ⁸¹ The (MTPPS^{4–}/Li⁺@C₆₀)_n films are composed of closely packed Li⁺@C₆₀ clusters of about 80 nm size, which render a nanoporous morphology to the film as shown in the TEM images in Fig. 4. ⁸¹

The photoelectrochemical measurements of a robust thin film of OTE/SnO $_2$ /(MTPPS 4 -/Li $^+$ @C $_{60}$) $_n$ were performed using a standard two-electrode system consisting of a working electrode and a Pt wire gauze electrode in air-saturated MeCN containing 0.5 M LiI and 0.01 M I $_2$ (Fig. 5). The IPCE (incident photon-to-photocurrent efficiency) values were determined by normalizing the photocurrent values for incident light energy and intensity and using eqn (1). $^{82-85}$

IPCE (%) =
$$100 \times 1240 \times i_{sc}/(I_{inc} \times \lambda)$$
 (1)

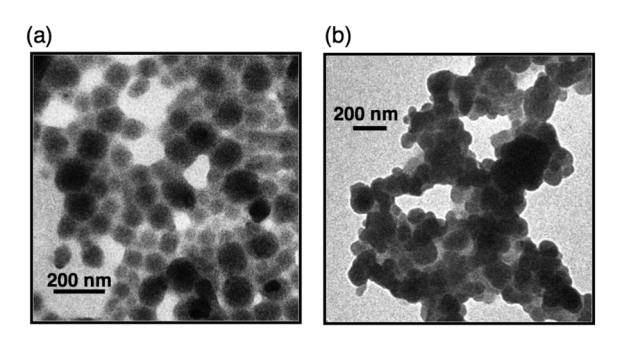


Fig. 4 TEM images of (a) Li⁺@ C_{60} /ZnTPPS⁴⁻ and (b) Li⁺@ C_{60} /H₂TPPS⁴⁻ nanoclusters.

Dalton Transactions Perspective

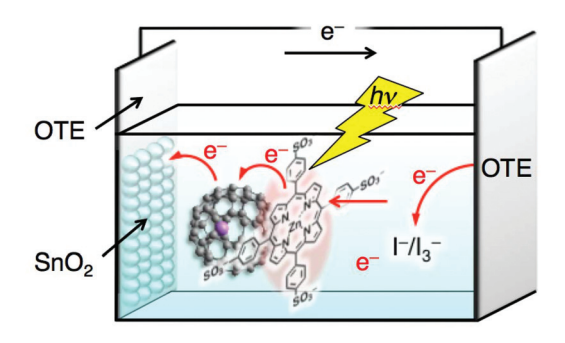


Fig. 5 Schematic image of photoelectrochemical cell of OTE/SnO₂/MTPPS⁴⁻/ Li⁺@C₆₀ and electron-transfer pathways to generate photocurrent.

where i_{sc} is the short circuit photocurrent (A cm⁻²), I_{inc} is the incident light intensity (W cm⁻²) and λ is the wavelength (nm). The IPCE value of $OTE/SnO_2/(ZnTPPS^4-/Li^+@C_{60})_n$ is much higher than the sum of the two individual IPCE values of the individual systems OTE/SnO₂/(ZnTPPS⁴⁻)_n and OTE/SnO₂/ $(Li^{\dagger} \otimes C_{60})_n$ in the visible region (Fig. 6). The maximum IPCE value of OTE/SnO₂/(ZnTPPS⁴⁻/Li⁺@C₆₀)_n was 77% at 450 nm. Such a high IPCE value indicates that photocurrent generation is initiated via photoinduced electron transfer from ZnTPPS⁴⁻ to Li⁺@C₆₀, followed by the charge transport to the collective surface of an OTE/SnO₂ electrode (Fig. 5). When ZnTPPS⁴⁻ was replaced by H2TPPS4-, a significantly low IPCE value was observed as 7% at 440 nm probably because of the self-aggregation of H₂TPPS⁴⁻ without binding with Li⁺@C₆₀.81

The power conversion efficiency (η) of the OTE/SnO₂/ $(ZnTPPS^{4-}/Li^{+}@C_{60})_n$ electrode was calculated by using eqn (2):82-85

$$\eta = FF \times I_{sc} \times V_{oc}/W_{in} \tag{2}$$

in which the fill factor (FF) is defined as FF = $[IV]_{max}/I_{sc}V_{oc}$ and $V_{\rm oc}$ is the open-circuit photovoltage and $I_{\rm sc}$ is the short-circuit photocurrent. The OTE/SnO₂/(ZnTPPS⁴⁻/Li⁺@C₆₀)_n electrode has an overall power conversion efficiency (η) of 2.1% at an input power ($W_{\rm in}$) of 28 mW cm⁻², whereas FF = 0.37, $V_{\rm oc}$ =

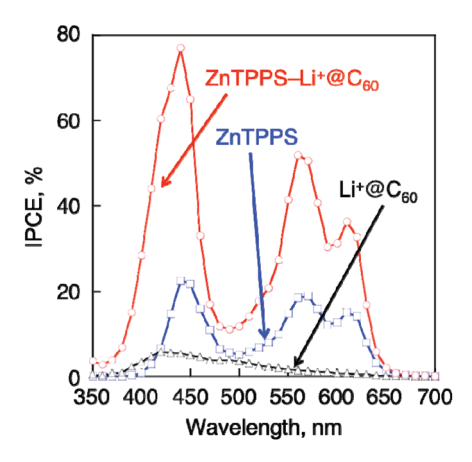


Fig. 6 Photocurrent action spectra of OTE/SnO₂/(ZnTPPS⁴⁻/Li⁺@C₆₀)_n, (red) $OTE/SnO_2/(ZnTPPS^{4-})_n$ (blue) and $OTE/SnO_2/(Li^+@C_{60})_n$ (black). Electrolyte: 0.5 M LiI and 0.01 M I_2 in MeCN-PhCN (3:1 v/v).

460 mV and $I_{sc} = 3.4 \text{ mA cm}^{-2}$ in the OTE/SnO₂/(ZnTPPS⁴⁻/ $\operatorname{Li}^{+}(\mathfrak{A}C_{60})_{n}$. The η value is two orders of magnitude greater than that of the previously reported simple porphyrin and C₆₀ composite system (~0.03%).83 Such a significant enhancement of the η value indicates that the strong ordering in the clusters and the efficient charge separation in (ZnTPPS⁴⁻/Li⁺@C₆₀)_n improved the light energy conversion properties.

Supramolecular complexes of cyclic porphyrin dimers with C₆₀ and Li⁺@C₆₀

As compared to porphyrin monomers, porphyrin dimers with appropriate linkage can accommodate electron acceptor guest by π - π interactions to form sandwich molecules complexes.86-96 For example, a cyclic Ni porphyrin dimer (Ni-CPD_{Pv}) linked by butadiyne moieties bearing 4-pyridyl groups (Fig. 7) forms a sandwich complex with C_{60} ($C_{60} \subset Ni_{2}$ -CPD_{Pv}) as shown in the X-ray crystal structure (Fig. 8), where the dimer bites a C₆₀ molecule by tilting the porphyrin rings with respect to each other and there are strong π – π interactions between the porphyrin rings and C₆₀.97 The adjacent dimers are linked by hydrogen bonds and π - π interactions. ⁹⁷ The C₆₀ molecules are linearly arranged in the inner channel to give a supramolecular peapod. 97-102

The linear arrangement of C₆₀ in C₆₀ ⊂ Ni₂-CPD_{Py} high electron mobilities of $\sum \mu = 0.72$ and 0.20 cm² V⁻¹ s⁻¹ along the b and c axes, respectively, which were determined by flashphotolysis time-resolved microwave conductivity (FP-TRMC) measurements.⁹⁷ The TRMC technique can evaluate the

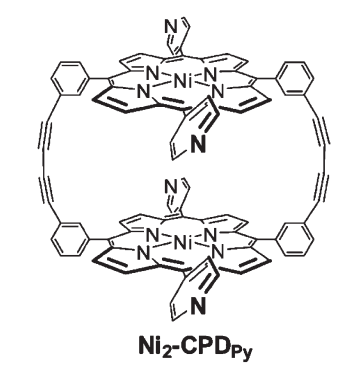


Fig. 7 Chemical structure of Ni₂-CPD_{Pv}

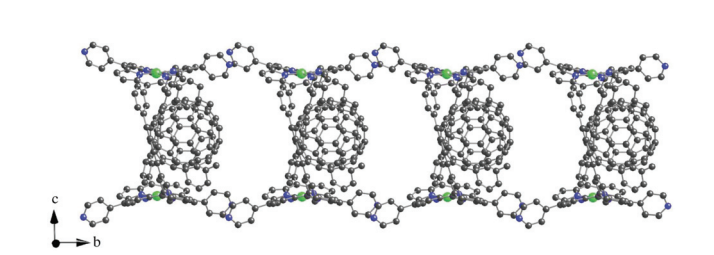


Fig. 8 Crystal structures of tubular assemblies of $C_{60} \subset Ni_2$ -CPD_{Pv}. Hydrogen atoms are omitted for clarity.

intrinsic mobility without being affected by the chemical or physical defects in the material and/or the organic/metal-electrode interfaces. $^{103-105}$ The observed value along the b axis of the single crystal of $C_{60} \subset Ni_2\text{-}CPD_{Py}$ is comparable to that of the single crystal of C_{60} ($\sum \mu = 0.50 \text{ cm}^2 \text{ V}^{-1} \text{ s}^{-1}$ measured by TOF). The observed high electron mobility along the b axis is due to the well-ordered linear arrangement of C₆₀ in the porphyrin nanotube. However, the expected charge-separated state could not be observed in the time-resolved transient absorption spectra of C₆₀ ⊂ Ni₂-CPD_{Pv} because the singlet excited state of the nickel porphyrin immediately changes to the triplet excited state by intersystem crossing and the low energy triplet excited state of C₆₀ (³C₆₀*) is formed by energy transfer.⁹⁷ The estimated energy level of the charge-separated state (1.98 eV) is higher than that of ${}^{3}C_{60}^{*}$ (1.60 eV). 97 When Ni₂-CPD_{Pv} was replaced by a free base porphyrin dimer (H4-CPDPy), a complete charge-separated state {H₄-CPDPy*+ +

 C_{60} \subset H_4 -CPD_{Py} in the solid state with a lifetime of 470 ps. 107 The photovoltaic activity of $C_{60} \subset Ni_2$ -CPD_{Py} and $C_{60} \subset H_4$ -CPD_{Py} was evaluated by using solar cells composed of modified electrodes and I^-/I_3^- solution. 107 The $C_{60} \subset H_4$ -CPD_{Py}-

modified electrode exhibited IPCE of 17% and a power conversion efficiency (η) of 0.33%, which was more than 16 times

larger than that of OTE/SnO₂/($C_{60} \subset Ni_2$ -CPD_{Pv})_n (0.02%). ¹⁰⁷

Such a significant enhancement of the η value demonstrates

that the formation of highly ordered clusters and the efficient

charge separation of $(C_{60} \subset H_4\text{-CPD}_{Py})_n$ contributes to the improvement of the light energy conversion properties. When C_{60} is replaced by $\text{Li}^+ @ C_{60}$, porphyrin dimers with four long alkoxy substituents on the *meso*-phenyl groups $(\text{MCPD}_{Py}(\text{OC}_6))$ in Fig. 9) form strong supramolecular complexes in even a polar solvent such as PhCN. The association constants (K_{assoc}) of $\text{Li}^+ @ C_{60} \subset \text{MCPD}_{Py}(\text{OC}_6)$ in PhCN at 298 K were determined to be $2.6 \times 10^5 \text{ M}^{-1}$ for $\text{Li}^+ @ C_{60} \subset \text{H}_4\text{-CPD}_{Py}(\text{OC}_6)$ and $3.5 \times 10^5 \text{ M}^{-1}$ for $\text{Li}^+ @ C_{60} \subset \text{Ni}_2\text{-CPD}_{Py}(\text{OC}_6)$.

Upon laser excitation of $\text{Li}^+@\text{C}_{60} \subset \text{Ni}_2\text{-CPD}_{\text{Py}}(\text{OC}_6)$, transient absorption bands due to $\text{Ni}_2\text{-CPD}_{\text{Py}}(\text{OC}_6)^{\text{r-}}$ and $\text{Li}^+@\text{C}_{60}^{\text{--}}$ were observed as shown in Fig. 10a. ¹⁰⁸ In this case, electron

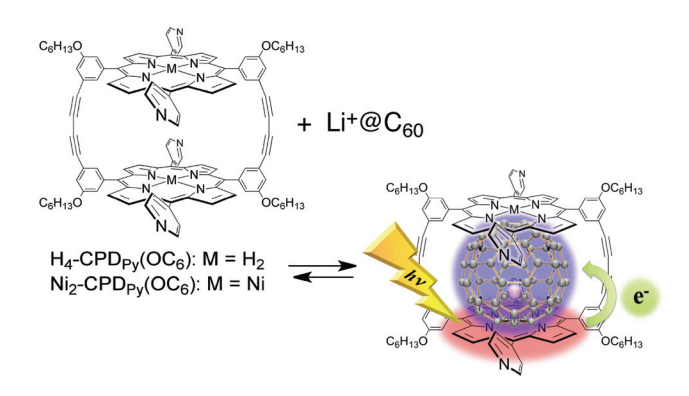
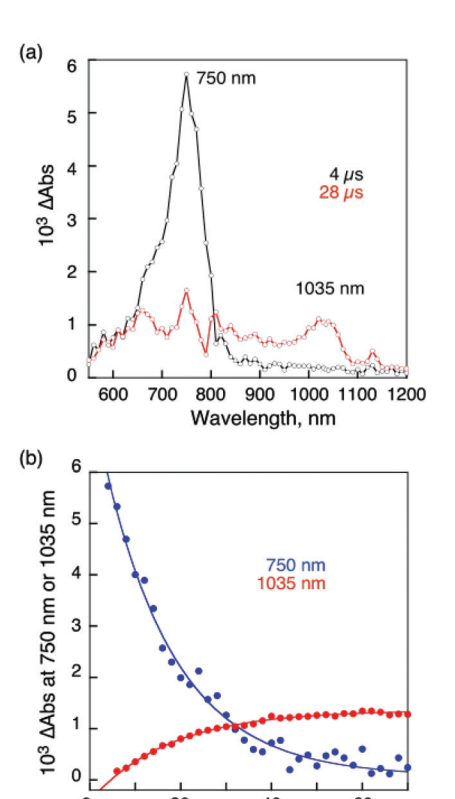


Fig. 9 Supramolecular formation and photoinduced charge separation between $MCPD_{PV}(OC_6)$ and $Li^+@C_{60}$.



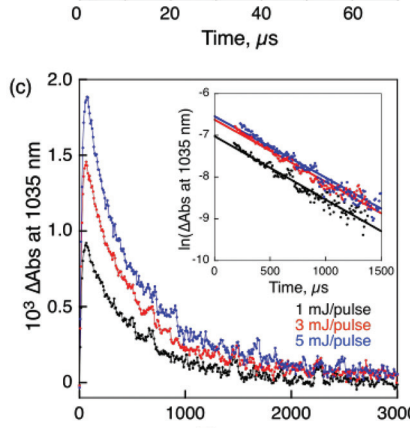
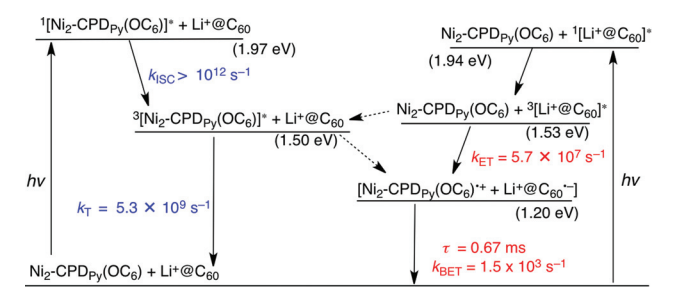


Fig. 10 (a) Transient absorption spectra of Ni₂-CPD_{Py}(OC₆) with Li⁺@C₆₀ in deaerated PhCN at room temperature taken at 4 and 28 μ s after nanosecond laser excitation at 520 nm. [Ni₂-CPD_{Py}(OC₆)] = 2.5 \times 10⁻⁵ M, [Li⁺@C₆₀] = 5.0 \times 10⁻⁵ M. (b) Rise and (c) decay time profiles at 1035 nm with different laser intensities (1, 3, 5 mJ per pluse). Inset: first-order plots.

transfer occurs from Ni₂-CPD_{Py}(OC₆) to the triplet excited state of Li⁺@C₆₀ (3 Li⁺@C₆₀*) rather than from 3 [Ni₂-CPD_{Py}(OC₆)]* to Li⁺@C₆₀ as indicated by the disappearance of the absorption band at 750 nm due to 3 Li⁺@C₆₀*, accompanied by the appearance of the absorption band at 1035 nm due to Li⁺@C₆₀*- (Fig. 10b). The rate constant of electron transfer from Ni₂-CPD_{Py}(OC₆) to 3 Li⁺@C₆₀* to produce the CS state was determined from the rise in the absorbance at 1035 nm due to Li⁺@C₆₀*- to be 5.7 × 10⁷ s⁻¹. The absorbance at 1035 nm due to Li⁺@C₆₀*- in the CS state decayed obeying first-order kinetics with the same slope irrespective of the difference in

Dalton Transactions



Scheme 2 Energy diagram for $Li^+@C_{60} \subset Ni_2\text{-CPD}_{Py}(OC_6)$; broken arrow: minor pathway.

the laser intensity (Fig. 10c). 108 This clearly indicates that the decay of the CS state occurs via intrasupramolecular back electron transfer rather than a bimolecular back electron-transfer reaction between the CS states. The CS lifetime was determined from the slope of the first-order plots in Fig. 10c to be 0.67 ms, which is the longest value ever reported for noncovalent monomer dimer porphyrin-fullerene supramolecules in solution. 108 The CS state was also observed for Li⁺(a)C₆₀ ⊂ H₄-CPD_{Pv}(OC₆). The quantum yields of the CS states were estimated to be 0.13 for $Li^+@C_{60} \subset Ni_2\text{-CPD}_{Pv}(OC_6)$ and 0.32 for $Li^{+} \otimes C_{60} \subset H_4\text{-CPD}_{Pv}(OC_6)$ and by means of the comparative method with the absorption intensities of the CS states $(\text{Li}^+ @\text{C}_{60}^{--}: \varepsilon(1035 \text{ nm}) = 7300 \text{ M}^{-1} \text{ cm}^{-1}).^{108} \text{ When Li}^+ @\text{C}_{60}$ was replaced by pristine C60, no CS states were produced as predicted by their higher energy levels than those of the triplet excited states of CPD_{Py}(OC₆) and C₆₀. 108

The mechanisms of intrasupramolecular photoinduced charge separation in $\operatorname{Li}^+(@C_{60} \subset \operatorname{Ni}_2\text{-}\operatorname{CPD}_{Py}(\operatorname{OC}_6)$ are shown in Scheme 2.¹⁰⁸ The singlet excited state of Ni₂-CPD_{Pv}(OC₆) (1[Ni₂-CPD_{Pv}(OC₆)]*) is generated upon photoexcitation of $Li^{+} @ C_{60} \subset Ni_{2}\text{-}CPD_{Pv}(OC_{6})$ at 420 nm, where the porphyrin moiety is exclusively excited. Even if the Li⁺@C₆₀ moiety is excited, energy transfer from ${}^{1}[Li^{+}@C_{60}]^{*}$ ($E_{s} = 1.94 \text{ eV}$)⁷⁷ to Ni_2 -CPD_{Pv}(OC₆) ($E_s = 1.97$ eV) occurs to produce $^{1}[Ni_{2}\text{-}CPD_{Pv}(OC_{6})]^{*}.$ Although electron transfer $^{1}[Ni_{2}\text{-}CPD_{Py}(OC_{6})]^{*}$ to $Li^{+}@C_{60}$ is energetically possible (Scheme 2), the fast intersystem crossing occurs to generate $^{3}[Ni_{2}\text{-CPD}_{Pv}(OC_{6})]^{*} (k_{ISC} > 10^{12} \text{ s}^{-1}).^{108} \text{ Then, electron transfer}$ occurs from ³[Ni₂-CPD_{Py}(OC₆)]* to Li⁺@C₆₀ with the driving force of 0.30 eV to produce the CS state. The CS state decays slowly via intrasupramolecular BET with the lifetime of 0.67 ms (Scheme 2).108

Supramolecular complex of a porphyrin tripod with C₆₀

The tripod conformation of a porphyrin trimer (TPZn₃) in Fig. 11 makes it possible to capture a fullerene derivative containing a pyridine moiety (PyC₆₀)¹⁰⁹ inside the cavity strongly by π - π interactions together with the coordination bond between Zn²⁺ and the pyridine moiety (Scheme 3).¹¹⁰⁻¹¹³ The association constant of $TPZn_3$ with $PyC_{60} \ (1.1 \times 10^5 \ M^{-1} \ in$

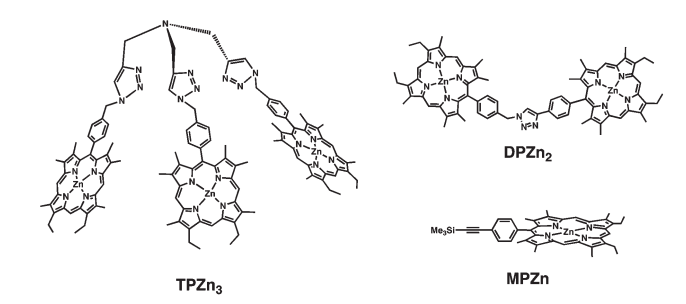


Fig. 11 A porphyrin tripod and the reference dimer and monomer.

$$\mathsf{TPZn}_3 + \mathsf{PyC}_{60} \xrightarrow{\mathsf{K}} (\mathsf{TPZn}_3 - \mathsf{PyC}_{60})$$

Scheme 3 Formation of a supramolecular complex between TPZn₃ and PyC₆₀.

toluene) determined from the UV-vis absorption spectral titration (Fig. 12a) is much larger as compared with those of the corresponding monomer (MPZn) and dimer porphyrin (DPZn₂).¹⁰⁹ The ¹H NMR signals of TPZn₃ exhibit downfield shifts upon complexation with PyC₆₀, whereas the pyridyl protons of PyC₆₀ exhibit large upfield shifts by the complexation, which is ascribed to the influence of the large porphyrin aromatic ring current. 113 This result clearly shows that the

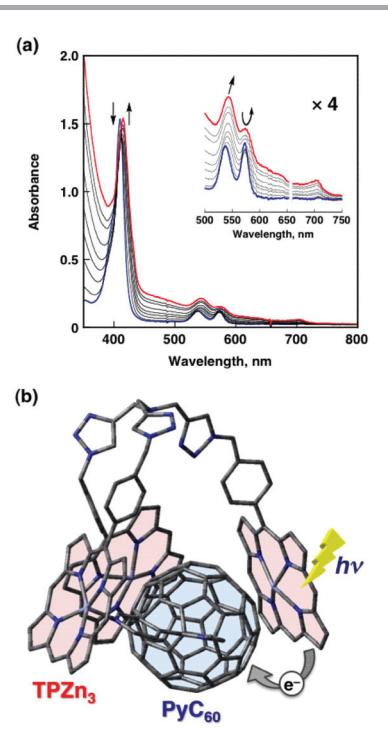


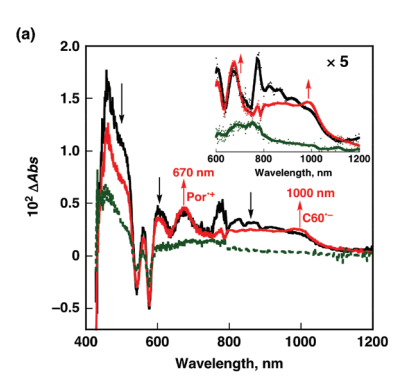
Fig. 12 (a) UV-Vis spectral changes upon addition of PyC_{60} (0 to 48 μM) to an o-DCB solution of TPZn $_3$ (3 μ M) at 298 K. (b) Schematic view of photoinduced electron transfer in the TPZn₃-PyC₆₀ complex. The structure of the TPZn₃-PyC₆₀ complex was optimized by DFT at the B3LYP/3-21G(*) level.

pyridyl group of PyC_{60} coordinates to the central zinc ions of $TPZn_3$. The encapsulation of PyC_{60} into the cavity of $TPZn_3$ was supported by the DFT-optimized structure (B3LYP/3-21G(*) basis set) in Fig. 12b. 113

The occurrence of photoinduced electron transfer from $^1\text{TPZn}_3{}^*$ to PyC_{60} was confirmed by femtosecond laser flash photolysis measurements in Fig. 13a, where the transient absorption spectrum due to $^1\text{TPZn}_3{}^*$ changes as time elapses to afford the absorption bands at $\lambda_{\text{max}}=1000$ nm due to the monofunctionalized fullerene radical anion 114,115 and at 670 nm due to the one-electron oxidized species of TPZn_3 (TPZn $_3{}^{*+}$). 113,116,117

In sharp contrast to the TPZn₃–PyC₆₀ complex, the transient absorption spectrum of the monomer porphyrin (MPZn) in the presence of PyC₆₀ (Fig. 13b) exhibits the absorbance change due to the energy transfer from $^1\text{MPZn*}$ to PyC₆₀ to give the singlet excited state $^1\text{PyC}_{60}^*$ (1.76 eV), followed by the conversion to the triplet excited states $^3\text{MPZn*}$ and $^3\text{PyC}_{60}^*$ at 2800 ps (green line in Fig. 13b), accompanied by the recovery of the ground state. 113

The energy diagrams of photodynamics for $TPZn_3$ and MPZn in the presence of PyC_{60} in toluene are shown in Scheme 4a and 4b, respectively. The energy level (1.49 eV) of the CS state ($TPZn_3^{*+}-PyC_{60}^{*-}$) is lower than the energy level of the triplet excited state of PyC_{60} moieties (1.56 eV). The rate constant ($k_{\rm ET}$) of photoinduce electron transfer from $^1TPZn_3^*$ to PyC_{60} is larger than the rate constant of intersystem crossing. From the rate constant of back electron transfer ($k_{\rm EET}$ =



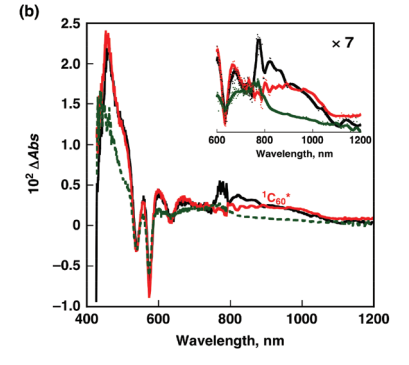
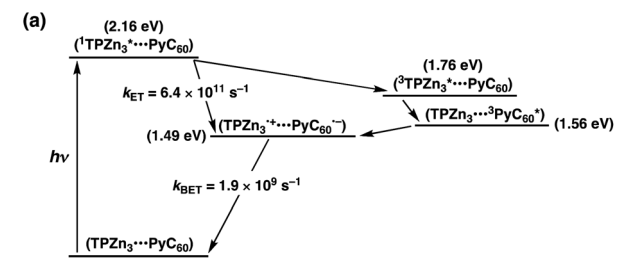
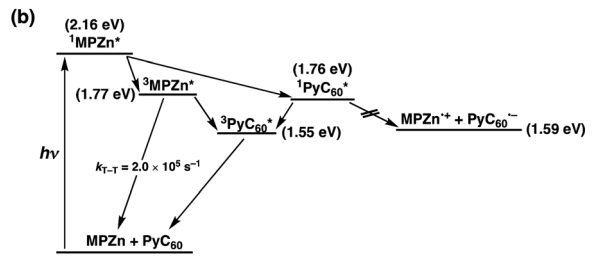


Fig. 13 Transient absorption spectra of (a) TPZn₃ $(7.0 \times 10^{-6} \text{ M})$ and (b) MPZn $(1.1 \times 10^{-5} \text{ M})$ in the presence of PyC₆₀ $(2.3 \times 10^{-5} \text{ M})$ obtained at 2 ps (black), 62 ps (red), and 2800 ps (green) after femtosecond laser pulse irradiation at 410 nm in deaerated toluene at 298 K.





Scheme 4 Energy diagrams for photodynamics of (a) $TPZn_3$ and (b) MPZn in the presence of PyC_{60} in toluene.

 $1.9 \times 10^9 \text{ s}^{-1}$), the lifetime of the CS state is determined to be $\tau_{\rm CS} = 0.53$ ns. In contrast, only energy transfer from $^1\text{MPZn*}$ to PyC₆₀ occurs to produce $^1\text{PyC}_{60}*$, in competition with intersystem crossing to $^3\text{MPZn*}.^{113}$

TPZn $_3$ also forms a stable 1:1 complex with gold(III) tetra(4-pyridyl)porphyrin (AuTPyP $^+$) in nonpolar solvents. 118 The strong binding of TPZn $_3$ with AuTPyP $^+$ results from the encapsulation of AuTPyP $^+$ inside the cavity of TPZn $_3$ through multiple coordination bonds. The efficient quenching of the singlet excited state of TPZn $_3$ occurs via a photoinduced electron-transfer pathway in the TPZn $_3$ -AuTPyP $^+$ complex as the case of TPZn $_3$ -PyC $_{60}$ complex. 118

5. Supramolecular complexes of porphyrin oligopeptides and C₆₀

Multiple photosynthetic reaction centres composed of light-harvesting multiporphyrin units and charge-separation units were obtained by using both the coordination bond and π – π interaction. Zinc porphyrinic oligopeptides with various numbers of porphyrin units $[P(ZnP)_n; n = 2, 4, 8]^{119,120}$ were used as light-harvesting multiporphyrin units (Fig. 14), which are bound to electron acceptors of fulleropyrrolidine bearing a pyridine $(PyC_{60})^{113}$ or imidazole coordinating ligand $(ImC_{60})^{82}$ as shown in Fig. 15. ¹²¹

The binding constant (K) of PyC₆₀ to P(ZnP)_n increased with increasing number of zinc porphyrins in an oligopeptide unit. ¹²¹ No supramolecular complex formation was observed in the case of zinc tetraphenylporphyrin in PhCN. ¹²¹ The strong binding between P(ZnP)₈ and PyC₆₀ results from the strong π - π interactions between two zinc porphyrins and PyC₆₀ in addition to the axial coordination of PyC₆₀ to zinc ions of the porphyrins. In the case of ImC₆₀, however, the highest K value was obtained in the P(ZnP)₄-ImC₆₀ complex. This

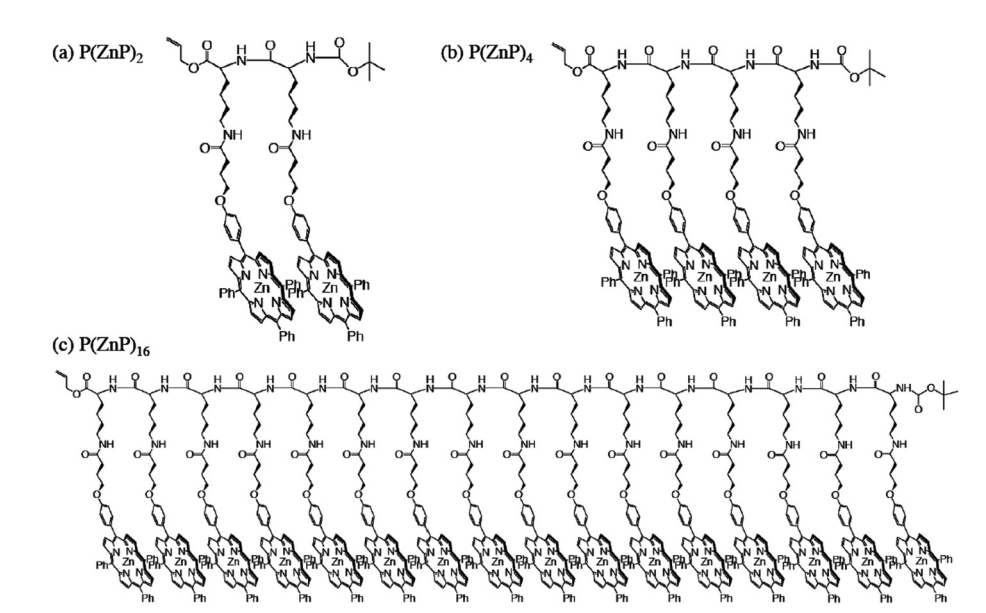


Fig. 14 Chemical structures of P(ZnP)₂, P(ZnP)₄ and P(ZnP)₁₆.

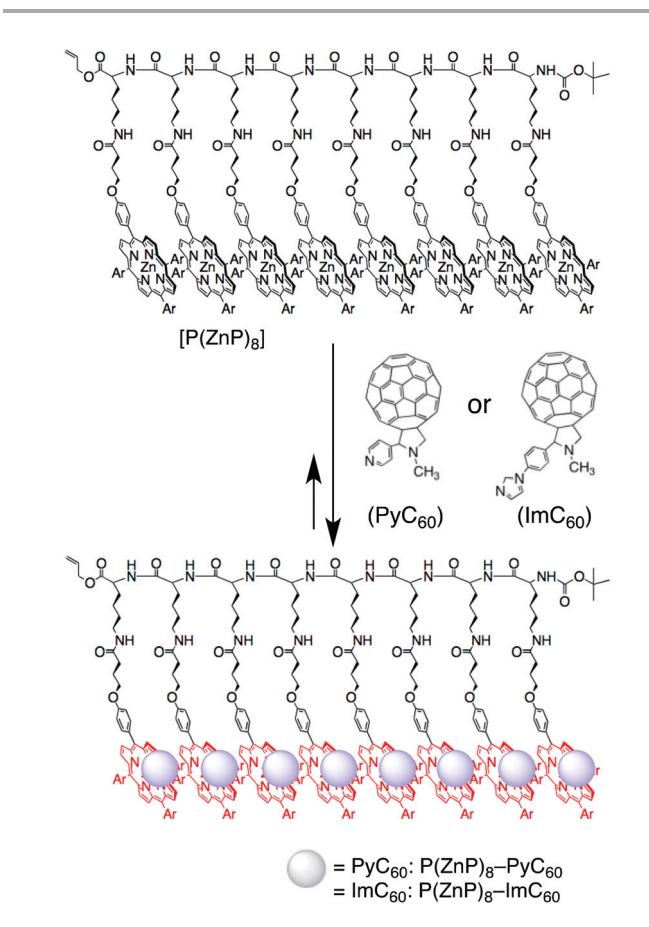


Fig. 15 Illustration of supramolecular complex composed of porphyrin-peptide octamer $[P(ZnP)_8, Ar = 3,5-(t-Bu)_2C_6H_3]$ and PyC_{60} or ImC_{60} .

indicates that ImC_{60} is much more strongly bound by the oligopeptide, $P(ZnP)_4$, than PyC_{60} . The apparent binding constants (K) determined from the fluorescence quenching of $P(ZnP)_n$ were significantly larger than those determined from

the UV-vis spectral change, and the difference in the values increased with increasing the generation of porphyrinic oligopeptides (with increasing the number of the porphyrin units). This indicates that the excited energy migration between the porphyrin units occurs efficiently prior to the electron transfer to the bound C_{60} moiety. An extremely efficient energy transfer also occurs in $P(ZnP)_8$ -Im C_{60} judging from the large difference in the K values determined by the absorption change and by the fluorescence quenching (1.5 × 10⁴ νs . 3.3 × 10⁵ M^{-1}).

The occurrence of photoinduced electron transfer in the supramolecular complex in PhCN was confirmed by the transient absorption spectra of the supramolecular complex of P(ZnP)₈ with PyC₆₀ using nanosecond laser flash photolysis. ¹²¹ The laser photoexcitation at 561 nm of the supramolecular complex of P(ZnP)₈ with PyC₆₀ results in formation of the CS state as indicated by the transient absorption spectra in Fig. 16a, where the absorption band due to PyC₆₀. is clearly observed at 1000 nm together with that due to ZnP*+ at 630 nm. 121 The CS state detected decays obeying first-order kinetics (Fig. 16b) and the first-order plots at different initial CS concentrations afford linear correlations with the same slope (inset of Fig. 16b). 121 If there is any contribution of intermolecular back electron transfer from unbound PyC₆₀*- to ZnP*+, the second-order kinetics would be involved for the decay time profile. In fact, the corresponding second-order plots (Fig. 16c) are clearly non-linear and the initial slope varies depending on the CS concentration. Thus, the decay process is ascribed to back electron transfer in the supramolecular complex rather than intermolecular back electron transfer between ZnP*+ and PyC60*-.121 The CS lifetimes of the supramolecular complexes of other porphyrins $[P(ZnP)_n]$ and the fullerene derivative (ImC₆₀) become longer with increasing generation of porphyrinic oligopeptides (with increasing the number of the porphyrin units). 121 Such elongation of the CS

Perspective

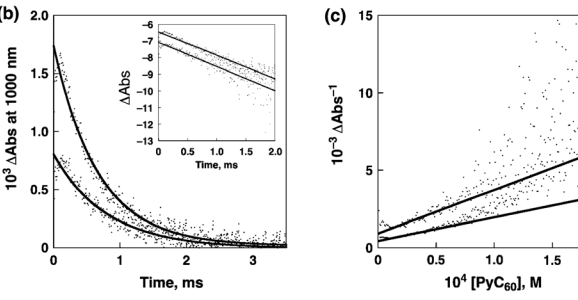


Fig. 16 (a) Transient absorption spectra of P(ZnP)₈ (2.9×10^{-6} M) in the presence of PyC₆₀ (4.9×10^{-3} M) in deaerated PhCN at 298 K taken at 70 (solid line with black circles) and 350 μs (solid line with white circles) after laser excitation at 561 nm (4 mJ per pulse), respectively. (b) Time profiles of the absorption at 1000 nm due to PyC₆₀* with different laser powers (4 and 1 mJ per pulse) at 298 K. Inset: first-order plots. (c) Second-order plots.

lifetimes results from efficient hole migration between the porphyrin units following the photoinduced electron transfer in the supramolecular complexes.

Multiple photosynthetic reaction centres have also been constructed using supramolecular complexes of zinc porphyrin dendrimers $[D(ZnP)_n: n = 4, 8, 16]$ with $PyC_{60}.^{122}$ Efficient energy migration occurs more efficiently between the ZnP units of dendrimers prior to the photoinduced electron transfer with increasing the generation of dendrimers to attain an extremely long CS lifetime *e.g.*, 0.25 ms for the $D(ZnP)_{16}-PyC_{60}$ complex in PhCN at 298 K. 122

Multiple photosynthetic reaction centres composed of supramolecular complexes of harvesting multiporphyrin units and charge-separation units have enabled us to construct supramolecular organic solar cells by the electrodeposition of mixed porphyrin-peptide oligomers $[P(H_2P)_n \text{ or } P(ZnP)_n]$ and C_{60} clusters $[(P(H_2P)_n + C_{60})_m$ or $(P(ZnP)_n + C_{60})_m]$ onto an optically transparent electrode (OTE) of a nanostructured SnO2 electrode (OTE/SnO2), to obtain modified electrodes [denoted as $(P(H_2P)_n + C_{60})_m$ or $(P(ZnP)_n + C_{60})_m$ (n = 1, 2, 4, 8, 16)]. The IPCE value increased with increasing the number of porphyrins in a polypeptide unit in both $(P(H_2P)_n + C_{60})_m$ and $(P(ZnP)_n + C_{60})_m$ (n = 1, 2, 4, 8, 16) systems as shown in Fig. 17. Such a good photoelectrochemical performance results from efficient photoinduced electron-transfer from the excited state of the porphyrin unit to C₆₀ in the supramolecular complex with longer CS lifetimes as the number of porphyrins in a polypeptide unit increases (vide supra). The maximum IPCE value of $(P(ZnP)_{16} + C_{60})_m$ (56%) is larger than that of $(P(H_2P)_{16} +$

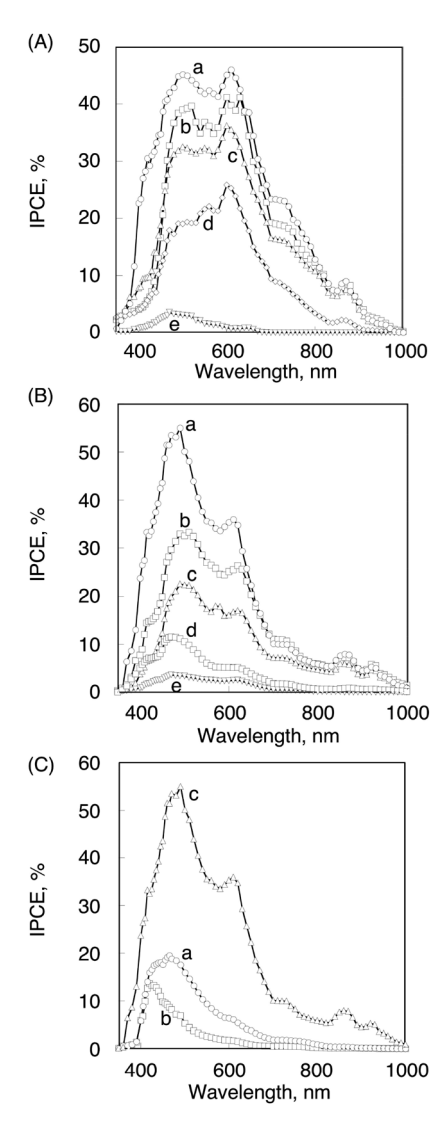
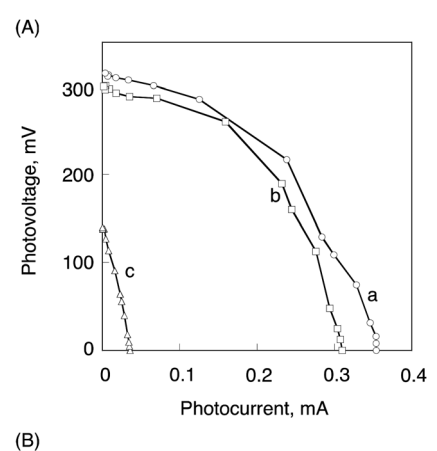


Fig. 17 (A) The photocurrent action spectra (IPCE vs. wavelength) of (a) $(P(H_2P)_{16} + C_{60})_m$, (b) $(P(H_2P)_8 + C_{60})_m$, (c) $(P(H_2P)_4 + C_{60})_m$, (d) $(P(H_2P)_2 + C_{60})_m$ and (e) $(P(H_2P)_1 + C_{60})_m$ modified OTE/SnO₂ electrodes. (B) The photocurrent action spectra of (a) $(P(ZnP)_{16} + C_{60})_m$, (b) $(P(ZnP)_8 + C_{60})_m$, (c) $(P(ZnP)_4 + C_{60})_m$, (d) $(P(ZnP)_2 + C_{60})_m$ and (e) $(P(ZnP)_1 + C_{60})_m$ modified electrodes. (C) The photocurrent action spectra of (a) $(P(ZnP)_{16} + ImC_{60})_m$, (b) $(P(ZnP)_{16} + PyC_{60})_m$ and (c) $(P(ZnP)_{16} + C_{60})_m$ modified OTE/SnO₂ electrodes. See text for the employed concentration of the individual species.

 C_{60} _m (48%) probably because of the larger driving force of the photoinduced electron transfer.

The maximum IPCE values of $(P(ZnP)_{16} + PyC_{60})_m$ (20%) and $(P(ZnP)_{16} + ImC_{60})_m$ (15%) are much smaller than that of $(P(ZnP)_{16} + C_{60})_m$ (56%), whereas the binding constant of $P(ZnP)_{16}-C_{60}$ is smaller than those of $P(ZnP)_{16}-ImC_{60}$ and $P(ZnP)_{16}-PyC_{60}$. The lower IPCE values of $P(ZnP)_{16}-ImC_{60}$ and $P(ZnP)_{16}-PyC_{60}$ systems as compared with that of $P(ZnP)_{16}-C_{60}$ system may result from the poor electron-transport properties of C_{60} derivatives due to the steric hindrance of the ligand moiety. Thus, a key element for efficient photocurrent generation is mainly the hole and electron transport in

Dalton Transactions Perspective



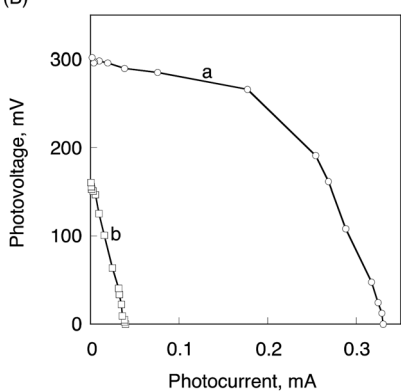


Fig. 18 (A) Current–voltage characteristics of (a) $(P(H_2P)_{16} + C_{60})_m$, (b) $(P(H_2P)_8)_m$ + C_{60} _m, and (c) $(P(H_2P)_1 + C_{60})_m$ modified electrodes. (B) Current-voltage characteristics of (a) $(P(ZnP)_{16} + C_{60})_m$ and (b) $(P(ZnP)_1 + C_{60})_m$. Electrolyte: 0.5 M Nal and 0.01 M I_2 in acetonitrile. Input power: 3.4 mW cm⁻², $\lambda > 400$ nm.

the thin film rather than the charge separation between porphyrins and C₆₀. 123

I/V characteristics of (a) $(P(H_2P)_{16} + C_{60})_m$, (b) $(P(H_2P)_8 + C_{60})_m$ $(C_{60})_m$ and (c) $(P(H_2P)_1 + C_{60})_m$ modified electrodes under visible light irradiation ($\lambda > 400$ nm) are shown in Fig. 18. The $(P(H_2P)_{16} + C_{60})_m$ system has a larger fill factor (FF) of 0.47, an open circuit voltage (V_{oc}) of 320 mV, a short circuit current density (I_{sc}) of 0.36 mA cm⁻², and the overall power conversion efficiency (η) of 1.6% at input power ($W_{\rm in}$) of 3.4 mW cm⁻². ¹²³

The η values of the $(P(H_2P)_{16} + C_{60})_m$ system was remarkably enhanced (around 40 times) in comparison with the $(P(H_2P)_1 +$ C_{60} _m modified electrode ($\eta = 0.043\%$) under the same experimental conditions. The η value of $(P(ZnP)_{16} + C_{60})_m$ is also determined as 1.4% and this value is much larger than that of $(P(ZnP)_1 + C_{60})_m (0.047\%)$ as shown in Fig. 18B. ¹²³

Conclusions

As described above, porphyrin monomers, dimers, trimers and oligomers form supramolecular complexes with fullerene derivatives via electrostatic interactions, π - π interactions and coordination bonds. Photoexcitation of the supramolecular complexes resulted in efficient photoinduced electron transfer from the porphyrin moiety to the fullerene moiety to produce

the long-lived CS states as revealed by laser flash photolysis measurements. In particular, a supramolecular complex of a cyclic Ni porphyrin dimer with Li⁺@C₆₀ [Li⁺@C₆₀ ⊂ Ni₂-CPD_{Pv}(OC₆)] affords a long-lived triplet CS state with 0.63 ms lifetime. A high IPCE value (77% at 450 nm) was achieved for a supramolecular solar cell using the OTE/SnO₂/(ZnTPPS⁴⁻/ $\operatorname{Li}^{+}(\mathfrak{Q}C_{60})_{n}$ electrode. The use of porphyrin oligomer peptides has also enabled to construct multiple photosynthetic reaction centres composed of light-harvesting multiporphyrin units and charge-separation units linked by both the coordination bond and π - π interactions, which afforded long-lived CS states. Supramolecular organic solar cells composed of porphyrinic oligopeptides and C60 exhibited higher overall power conversion efficiency with increasing the number of porphyrin units. Supramolecular complexes formed between porphyrins and fullerenes in particular Li⁺@C₆₀ provide promising materials for more efficient solar energy conversion.

Acknowledgements

The authors gratefully acknowledge the contributions of their collaborators and co-workers mentioned in the cited references, in particular Prof. Fumito Tani (Kyushu University) and Prof. Taku Hasobe (Keio University). Financial supports from the Grants-in-Aid (no. 20108010 to S.F. and 23750014 to K.O.) from MEXT of Japan and KOSEF/MEST of Korea through WCU project (R31-2008-000-10010-0) are gratefully acknowledged.

References

- 1 Anoxygenic Photosynthetic Bacteria, ed. R. E. Blankenship, M. T. Madigan and C. E. Bauer, Kluwer Academic Publishers, Dordrecht, The Netherlands, 1995.
- 2 W. Leibl and P. Mathis, in Electron Transfer in Photosynthesis. Series on Photoconversion of Solar Energy, 2004, vol. 2, p. 117.
- 3 T. A. Faunce, W. Lubitz, A. W. Rutherford, D. MacFarlane, G. F. Moore, P. Yang, D. G. Nocera, T. A. Moore, D. H. Gregory, S. Fukuzumi, K. B. Yoon, F. A. Armstrong, M. R. Wasielewski and S. Styring, Energy Environ. Sci., 2013, 6, 695.
- 4 S. Fukuzumi, Y. Yamada, T. Suenobu, K. Ohkubo and H. Kotani, Energy Environ. Sci., 2011, 4, 2754.
- 5 A. Harriman and J.-P. Sauvage, Chem. Soc. Rev., 1996, 25, 41.
- 6 M. N. Paddon-Row, Adv. Phys. Org. Chem., 2003, 38, 1.
- 7 M. N. Paddon-Row, Acc. Chem. Res., 1994, 27, 18.
- 8 D. Gust, T. A. Moore and A. L. Moore, Acc. Chem. Res., 2009, 42, 1890.
- 9 D. Gust, T. A. Moore and A. L. Moore, Faraday Discuss., 2012, 155, 9.
- 10 M. R. Wasielewski, Acc. Chem. Res., 2009, 42, 1910.
- 11 C. Thilgen and F. Diederich, Chem. Rev., 2006, 106, 5049.
- 12 F. Giacalone and N. Martín, Chem. Rev., 2006, 106, 5136.

- 13 W.-S. Li and T. Aida, Chem. Rev., 2009, 109, 6047.
- 14 C. M. Drain, A. Varotto and I. Radivojevic, Chem. Rev., 2009, 109, 1630.
- 15 (a) F. D'Souza and O. Ito, Coord. Chem. Rev., 2005, 249, 1410; (b) F. D'Souza and O. Ito, Chem. Commun., 2009, 4913; (c) F. D'Souza, A. S. D. Sandanayaka and O. Ito, J. Phys. Chem. Lett., 2010, 1, 2586; (d) F. D'Souza and O. Ito, Chem. Soc. Rev., 2012, 41, 86.
- 16 (a) S. Fukuzumi, Bull. Chem. Soc. Jpn., 2006, 79, 177; (b) S. Fukuzumi, Phys. Chem. Chem. Phys., 2008, 10, 2283; (c) S. Fukuzumi, Pure Appl. Chem., 2007, 79, 981; (d) S. Fukuzumi, Org. Biomol. Chem., 2003, 1, 609.
- 17 H. Imahori and S. Fukuzumi, Adv. Funct. Mater., 2004, 14,
- 18 D. M. Guldi, G. M. A. Rahman, F. Zerbetto and M. Prato, Acc. Chem. Res., 2005, 38, 871.
- 19 G. Bottari, G. de la Torre, D. M. Guldi and T. Torres, Chem. Rev., 2010, 110, 676.
- 20 S. Fukuzumi, T. Honda, K. Ohkubo and T. Kojima, Dalton Trans., 2009, 3880.
- 21 S. Fukuzumi and T. Kojima, J. Mater. Chem., 2008, 18,
- 22 D. M. Guldi and V. Sgobba, Chem. Commun., 2011, 47,
- 23 D. M. Guldi, Phys. Chem. Chem. Phys., 2007, 9, 1400.
- 24 S. Fukuzumi and K. Ohkubo, J. Mater. Chem., 2012, 22,
- 25 (a) K. Ohkubo and S. Fukuzumi, J. Porphyrins Phthalocyanines, 2008, 12, 993; (b) K. Ohkubo and S. Fukuzumi, Bull. Chem. Soc. Jpn., 2009, 82, 303.
- 26 G. Bottari, G. de la Torre, D. M. Guldi and T. Torres, Chem. Rev., 2010, 110, 6768.
- 27 M. V. Martinez-Diaz, N. S. Fender, M. S. Rodriguez-Morgade, M. Gomez-Lopez, F. Diederich, L. Echegoyen, J. F. Stoddart and T. Torres, J. Mater. Chem., 2002, 12, 2095.
- 28 (a) C. G. Claessens and T. Torres, Chem. Commun., 2004, 1298; (b) C. G. Claessens and T. Torres, J. Am. Chem. Soc., 2002, 124, 14522.
- 29 S. Fukuzumi, K. Ohkubo, F. D'Souza and J. L. Sessler, Chem. Commun., 2012, 48, 9801.
- 30 J.-F. Nierengarten, U. Hahn, T. M. F. Duarte, F. Cardinali, N. Solladié, M. E. Walther, A. Van Dorsselaer, H. Herschbach, E. Leize, A.-M. Albrecht-Gary, A. Trabolsi and M. Elhabiri, C. R. Chim., 2006, 9, 1022.
- 31 L. Echegoyen, F. Diederich and L. E. Echegoyen, in Fullerenes: Chemistry, Physics and Technology, ed. K. M. Kadish and R. S. Ruoff, Wiley-Interscience, New York, 2000, pp. 1-51.
- 32 T. M. Figueira-Duarte, A. Gegout and J.-F. Nierengarten, Chem. Commun., 2007, 109.
- 33 S. Fukuzumi and D. M. Guldi, in Electron Transfer in Chemistry, ed. V. Balzani, Wiley-VCH, Weinheim, 2001, vol. 2, pp. 270-337.
- 34 S. Fukuzumi, in Functional Organic Materials, ed. T. J. J. Müller and U. H. F. Bunz, Wiley-VCH, 2007, pp. 465–510.

- 35 J.-F. Nierengarten, New J. Chem., 2004, 28, 1177.
- 36 S. Fukuzumi, I. Nakanishi, T. Suenobu and K. M. Kadish, J. Am. Chem. Soc., 1999, 121, 3468.
- 37 S. Fukuzumi, K. Ohkubo, H. Imahori and D. M. Guldi, Chem.-Eur. J., 2003, 9, 1585.
- 38 Y. Kawashima, K. Ohkubo and S. Fukuzumi, I. Phys. Chem. A, 2013, 117, 6737.
- 39 S. Fukuzumi, K. Ohkubo, H. Imahori, J. Shao, Z. Ou, G. Zheng, Y. Chen, R. K. Pandey, M. Fujitsuka, O. Ito and K. M. Kadish, J. Am. Chem. Soc., 2001, 123, 10676.
- 40 D. Wróbel and A. Graja, Coord. Chem. Rev., 2011, 255, 2555.
- 41 H. Imahori, K. Tamaki, D. M. Guldi, C. Luo, M. Fujitsuka, O. Ito, Y. Sakata and S. Fukuzumi, J. Am. Chem. Soc., 2001, **123**, 2607.
- 42 H. Imahori, D. M. Guldi, K. Tamaki, Y. Yoshida, C. Luo, Y. Sakata and S. Fukuzumi, J. Am. Chem. Soc., 2001, 123,
- 43 K. Ohkubo, H. Imahori, J. Shao, Z. Ou, K. M. Kadish, Y. Chen, G. Zheng, R. K. Pandey, M. Fujitsuka, O. Ito and S. Fukuzumi, J. Phys. Chem. A, 2002, 106, 10991.
- 44 H. Imahori, K. Tamaki, Y. Araki, Y. Sekiguchi, O. Ito, Y. Sakata and S. Fukuzumi, J. Am. Chem. Soc., 2002, 124, 5165.
- 45 K. Ohkubo, H. Kotani, J. Shao, Z. Ou, K. M. Kadish, G. Li, R. K. Pandey, M. Fujitsuka, O. Ito, H. Imahori and S. Fukuzumi, Angew. Chem., Int. Ed., 2004, 43, 853.
- 46 F. D'Souza, P. M. Smith, M. E. Zandler, A. L. McCarty, M. Itou, Y. Araki and O. Ito, J. Am. Chem. Soc., 2004, 126, 7898.
- 47 H. Imahori, Y. Sekiguchi, Y. Kashiwagi, T. Sato, Y. Araki, O. Ito, H. Yamada and S. Fukuzumi, Chem.-Eur. J., 2004, 10, 3184.
- 48 F. D'Souza, R. Chitta, S. Gadde, S. D.-M. Islam, A. L. Schumacher, M. E. Zandler, Y. Araki and O. Ito, J. Phys. Chem. B, 2006, 110, 25240.
- 49 F. D'Souza, R. Chitta, S. Gadde, L. M. Rogers, P. A. Karr, M. E. Zandler, A. S. D. Sandanayaka, Y. Araki and O. Ito, Chem.-Eur. J., 2007, 13, 916.
- 50 R. Chitta, K. Ohkubo, M. Tasior, N. K. Subbaiyan, M. E. Zandler, D. T. Gryko, S. Fukuzumi and F. D'Souza, J. Am. Chem. Soc., 2008, 130, 14263.
- 51 F. D'Souza, E. Maligaspe, P. A. Karr, A. L. Schumacher, M. El Ojaimi, C. P. Gros, J.-M. Barbe, K. Ohkubo and S. Fukuzumi, Chem.-Eur. J., 2008, 14, 674.
- 52 F. D'Souza, E. Maligaspe, K. Ohkubo, M. E. Zandler, N. K. Subbaiyan and S. Fukuzumi, J. Am. Chem. Soc., 2009, 131, 8787.
- 53 F. D'Souza, G. M. Venukadasula, K. Yamanaka, N. K. Subbaiyan, M. E. Zandler and O. Ito, Org. Biomol. Chem., 2009, 7, 1076.
- 54 F. D'Souza, N. K. Subbaiyan, Y. Xie, J. P. Hill, K. Ariga, K. Ohkubo and S. Fukuzumi, J. Am. Chem. Soc., 2009, 131, 16138.
- 55 E. Maligaspe, T. Kumpulainen, N. K. Subbaiyan, M. E. Zandler, H. Lemmetyinen, N. V. Tkachenko and F. D'Souza, Phys. Chem. Chem. Phys., 2010, 12, 7434.

56 M. E. El-Khouly, D. K. Ju, K.-Y. Kay, F. D'Souza and S. Fukuzumi, *Chem.–Eur. J.*, 2010, **16**, 6193.

Dalton Transactions

- 57 F. D'Souza, C. A. Wijesinghe, M. E. El-Khouly, J. Hudson, M. Niemi, H. Lemmetyinen, N. V. Tkachenko, M. E. Zandler and S. Fukuzumi, *Phys. Chem. Chem. Phys.*, 2011, 13, 18168.
- 58 F. D'Souza, A. N. Amin, M. E. El-Khouly, N. K. Subbaiyan, M. E. Zandler and S. Fukuzumi, J. Am. Chem. Soc., 2012, 134, 654.
- 59 S.-H. Lee, A. G. Larsen, K. Ohkubo, J. R. Reimers, S. Fukuzumi and M. J. Crossley, *Chem. Sci.*, 2012, 3, 257.
- 60 V. Garg, G. Kodis, M. Chachisvilis, M. Hambourger, A. L. Moore, T. A. Moore and D. Gust, *J. Am. Chem. Soc.*, 2011, 133, 2944.
- 61 J. Frey, G. Kodis, S. D. Straight, T. A. Moore, A. L. Moore and D. Gust, *J. Phys. Chem. A*, 2013, **117**, 607.
- 62 Y. Kashiwagi, K. Ohkubo, J. A. McDonald, I. M. Blake, M. J. Crossley, Y. Araki, O. Ito, H. Imahori and S. Fukuzumi, *Org. Lett.*, 2003, 5, 2719.
- 63 D. Curiel, K. Ohkubo, J. R. Reimers, S. Fukuzumi and M. J. Crossley, *Phys. Chem. Chem. Phys.*, 2007, **9**, 5260.
- 64 J. Iehl, M. Vartanian, M. Holler, J.-F. Nierengarten, B. Delavaux-Nicot, J.-M. Strub, A. Van Dorsselaer, Y. Wu, J. Mohanraj, K. Yoosaf and N. Armaroli, *J. Mater. Chem.*, 2011, 21, 1562.
- 65 F. D'Souza, G. R. Deviprasad, M. S. Rahman and J.-P. Choi, *Inorg. Chem.*, 1999, 38, 2157.
- 66 F. D'Souza, G. R. Deviprasad, M. E. Zandler, V. T. Hoang, A. Klykov, M. VanStipdonk, A. Perera, M. E. El-Khouly, M. Fujitsuka and O. Ito, *J. Phys. Chem.* A, 2002, 106, 3243.
- 67 T. Da Ros, M. Prato, D. M. Guldi, M. Ruzzi and L. Pasimeni, *Chem.–Eur. J.*, 2001, 7, 816.
- 68 F. D'Souza, G. R. Deviprasad, M. E. El-Khouly, M. Fujitsuka and O. Ito, *J. Am. Chem. Soc.*, 2001, 123, 5277.
- 69 T. Honda, T. Nakanishi, K. Ohkubo, T. Kojima and S. Fukuzumi, *J. Am. Chem. Soc.*, 2010, **132**, 10155.
- 70 T. Honda, T. Kojima, N. Kobayashi and S. Fukuzumi, *Angew. Chem., Int. Ed.*, 2011, **50**, 2725.
- 71 S. Fukuzumi, T. Honda and T. Kojima, *Coord. Chem. Rev.*, 2012, **256**, 2488.
- 72 J. L. Sessler, E. Karnas, S. K. Kim, Z. Ou, M. Zhang, K. M. Kadish, K. Ohkubo and S. Fukuzumi, *J. Am. Chem. Soc.*, 2008, **130**, 15256.
- 73 E. Karnas, S. K. Kima, K. A. Johnson, J. L. Sessler, K. Ohkubo and S. Fukuzumi, *J. Am. Chem. Soc.*, 2010, **132**, 16617.
- 74 S. Aoyagi, E. Nishibori, H. Sawa, K. Sugimoto, M. Takata, Y. Miyata, R. Kitaura, H. Shinohara, H. Okada, T. Sakai, Y. Ono, K. Kawachi, K. Yokoo, S. Ono, K. Omote, Y. Kasama, S. Ishikawa, T. Komuro and H. Tobita, *Nat. Chem.*, 2010, 4, 678.
- 75 S. Fukuzumi, K. Ohkubo, Y. Kawashima, D. S. Kim, J. S. Park, A. Jana, V. Lynch, D. Kim and J. L. Sessler, J. Am. Chem. Soc., 2011, 133, 15938.

- 76 N. L. Bill, M. Ishida, S. Bähring, J. M. Lim, S. Lee, C. M. Davis, V. M. Lynch, K. A. Nielsen, J. O. Jeppesen, K. Ohkubo, S. Fukuzumi, D. Kim and J. L. Sessler, *J. Am. Chem. Soc.*, 2013, 135, 10852.
- 77 Y. Kawashima, K. Ohkubo and S. Fukuzumi, *J. Phys. Chem. A*, 2012, **116**, 8942.
- 78 K. Ohkubo, Y. Kawashima and S. Fukuzumi, *Chem. Commun.*, 2012, 48, 4314.
- 79 J. S. Park, E. Karnas, K. Ohkubo, P. Chen, K. M. Kadish, S. Fukuzumi, C. W. Bielawski, T. W. Hudnall, V. M. Lynch and J. L. Sessler, *Science*, 2010, 329, 1324.
- 80 M. Murakami, K. Ohkubo, T. Nanjo, K. Souma, N. Suzuki and S. Fukuzumi, *ChemPhysChem*, 2010, **11**, 2594.
- 81 K. Ohkubo, Y. Kawashima, H. Sakai, T. Hasobe and S. Fukuzumi, *Chem. Commun.*, 2013, **49**, 4474.
- 82 T. Hasobe, Y. Kashiwagi, M. A. Absalom, J. Sly, K. Hosomizu, M. J. Crossley, H. Imahori, P. V. Kamat and S. Fukuzumi, *Adv. Mater.*, 2004, **16**, 975.
- 83 T. Hasobe, H. Imahori, S. Fukuzumi and P. V. Kamat, *J. Phys. Chem. B*, 2003, **107**, 12105.
- 84 T. Hasobe, H. Imahori, P. V. Kamat, T. K. Ahn, D. Kim, T. Hanada, T. Hirakawa and S. Fukuzumi, *J. Am. Chem. Soc.*, 2005, 127, 1216.
- 85 T. Hasobe, P. V. Kamat, V. Troiani, N. Solladié, T. K. Ahn, S. K. Kim, D. Kim, A. Kongkanand, S. Kuwabata and S. Fukuzumi, J. Phys. Chem. B, 2005, 109, 19.
- 86 D. Sun, F. S. Tham, C. A. Reed, L. Chaker, M. Burgess and P. D. W. Boyd, *J. Am. Chem. Soc.*, 2000, 122, 10704.
- 87 D. Sun, F. S. Tham, C. A. Reed, L. Chaker and P. D. W. Boyd, *J. Am. Chem. Soc.*, 2002, **124**, 6604.
- 88 M. Tanaka, K. Ohkubo, C. P. Gros, R. Guilard and S. Fukuzumi, *J. Am. Chem. Soc.*, 2006, **128**, 14625.
- 89 L. P. Hernández-Eguía, E. C. Escudero-Adán, I. C. Pintre, B. Ventura, L. Flamigni and P. Ballester, *Chem.-Eur. J.*, 2011, 17, 14564.
- 90 A. L. Kieran, S. I. Pascu, T. Jarrosson and J. K. M. Sanders, *Chem. Commun.*, 2005, 1276.
- 91 B. Grimm, J. Schornbaum, C. M. Cardona, J. D. van Paauwe, P. D. W. Boyd and D. M. Guldi, *Chem. Sci.*, 2011, 2, 1530.
- 92 L. P. Hernández-Eguía, E. C. Escudero-Adán, J. R. Pinzón, L. Echegoyen and P. Ballester, *J. Org. Chem.*, 2011, 76, 3258.
- 93 S. K. Samanta and M. Schmittel, *Org. Biomol. Chem.*, 2013, 11, 3108.
- 94 K. Börjesson, J. G. Woller, E. Parsa, J. Mårtensson and B. Albinsson, *Chem. Commun.*, 2012, 48, 1793.
- B. Kang, R. K. Totten, M. H. Weston, J. T. Hupp and S. T. Nguyen, *Dalton Trans.*, 2012, 41, 12156.
- 96 S. Fukuzumi, I. Amasaki, K. Ohkubo, C. P. Gros, R. Guilard and J.-M. Barbe, *RSC Adv.*, 2012, 2, 3741.
- 97 H. Nobukuni, F. Tani, Y. Shimazaki, Y. Naruta, K. Ohkubo, T. Nakanishi, T. Kojima, S. Fukuzumi and S. Seki, J. Phys. Chem. C, 2009, 113, 19694.
- 98 T. Yamaguchi, N. Ishii, K. Tashiro and T. Aida, *J. Am. Chem. Soc.*, 2003, **125**, 13934.

99 R. Harada, Y. Matsuda, H. Okawa and T. Kojima, Angew.

- Chem., Int. Ed., 2004, 43, 1825.
- 100 T. Kojima, T. Nakanishi, R. Harada, K. Ohkubo, S. Yamauchi and S. Fukuzumi, *Chem.-Eur. J.*, 2007, **13**, 8714.
- 101 T. Nakanishi, T. Kojima, K. Ohkubo, T. Hasobe, K. Nakayama and S. Fukuzumi, *Chem. Mater.*, 2008, 20, 7492.
- 102 T. Kojima, R. Harada, T. Nakanishi, K. Kaneko and S. Fukuzumi, *Chem. Mater.*, 2007, **19**, 51.
- 103 A. Saeki, Y. Koizumi, T. Aida and S. Seki, Acc. Chem. Res., 2012, 45, 1193.
- 104 R. J. O. M. Hoofman, M. P. de Hass, L. D. A. Siebbeles and J. M. Warman, *Nature*, 1998, 392, 54.
- 105 J. H. Choi, T. Honda, S. Seki and S. Fukuzumi, *Chem. Commun.*, 2011, 47, 11213.
- 106 E. Frankevich, Y. Maruyama and H. Ogata, *Chem. Phys. Lett.*, 1993, 214, 39.
- 107 H. Nobukuni, Y. Shimazaki, H. Uno, Y. Naruta, K. Ohkubo, T. Kojima, S. Fukuzumi, S. Seki, H. Sakai, T. Hasobe and F. Tani, *Chem.–Eur. J.*, 2010, **16**, 11611.
- 108 T. Kamimura, K. Ohkubo, Y. Kawashima, H. Nobukuni, Y. Naruta, F. Tani and S. Fukuzumi, *Chem. Sci.*, 2013, 4, 1451.
- 109 F. D'Souza, P. M. Smith, S. Gadde, A. L. McCarty, M. J. Kullman, M. E. Zandler, M. Itou, Y. Araki and O. Ito, *J. Phys. Chem. B*, 2004, 108, 11333.
- 110 N. Armaroli, F. Diederich, L. Echegoyen, T. Habicher, L. Flamigni, G. Marconi and J.-F. Nierengarten, *New J. Chem.*, 1999, 77.
- 111 T. Da Ros, M. Prato, D. M. Guldi, E. Alessio, M. Ruzzi and L. Pasimeni, *Chem. Commun.*, 1999, 635.

- 112 F. Hauke, A. Swartz, D. M. Guldi and A. Hirsch, J. Mater. Chem., 2002, 12, 2088.
- 113 A. Takai, M. Chkounda, A. Eggenspiller, C. P. Gros, M. Lachkar, J.-M. Barbe and S. Fukuzumi, *J. Am. Chem. Soc.*, 2010, 132, 4477.
- 114 F. D'Souza, G. R. Deviprasad, M. E. Zandler, V. T. Hoang, A. Klykov, M. VanStipdonk, A. Perera, M. E. El-Khouly, M. Fujitsuka and O. Ito, J. Phys. Chem. A, 2002, 106, 3243.
- 115 D. I. Schuster, K. Loa, D. M. Guldi, A. Palkar, L. Echegoyen, C. Stanisky, R. J. Cross, M. Niemi, M. V. Tkachenko and H. Lemmetyinen, *J. Am. Chem. Soc.*, 2007, 129, 15973.
- 116 A. Takai, C. P. Gros, R. Guilard and S. Fukuzumi, *Chem.-Eur. J.*, 2009, **15**, 3110.
- 117 A. Takai, C. P. Gros, J.-M. Barbe and S. Fukuzumi, *Chem.-Eur. J.*, 2011, 17, 3420.
- 118 A. Takai, C. P. Gros, J.-M. Barbe and S. Fukuzumi, *Phys. Chem. Chem. Phys.*, 2010, **12**, 12160.
- 119 N. Solladié, A. Hamel and M. Gross, Tetrahedron Lett., 2000, 41, 6075.
- 120 F. Aziat, R. Rein, J. Peon, E. Rivera and N. Solladié, *J. Porphyrins Phthalocyanines*, 2008, **12**, 1232.
- 121 S. Fukuzumi, K. Saito, K. Ohkubo, V. Troiani, H. Qiu, S. Gadde, F. D'Souza and N. Solladié, *Phys. Chem. Chem. Phys.*, 2011, 13, 17019.
- 122 S. Fukuzumi, K. Saito, K. Ohkubo, T. Khoury, Y. Kashiwagi, M. A. Absalom, S. Gadde, F. D'Souza, Y. Araki, O. Ito and M. J. Crossley, *Chem. Commun.*, 2011, 47, 7980.
- 123 T. Hasobe, K. Saito, P. V. Kamat, V. Troiani, H. Qiu, N. Solladié, T. K. Ahn, K. S. Kim, S. K. Kim, D. Kim, F. D'Souza and S. Fukuzumi, J. Mater. Chem., 2007, 17, 4160.